

Molecular Pathogenesis of Genetic and Inherited Diseases

Aminoacyl-tRNA Synthetase-Interacting Multifunctional Protein 1/p43 Controls Endoplasmic Reticulum Retention of Heat Shock Protein gp96

Its Pathological Implications in Lupus-Like Autoimmune Diseases

Jung Min Han,* Sang Gyu Park,[†] Bei Liu,[‡] Bum-Joon Park,[†] Jin Young Kim,[†] Cheng He Jin,[†] Yeong Wook Song,[§] Zihai Li,[‡] and Sunghoon Kim[†]

From Imagen Company Biotechnology Incubating Center,* Golden Helix, the National Creative Research Initiatives Center for Aminoacyl-tRNA Synthetase Network,[†] College of Pharmacy, and the Department of Internal Medicine,[§] National Research Laboratory for Rheumatic Diseases, College of Medicine, Seoul National University, Seoul, Korea; and the Center for Immunotherapy of Cancer and Infectious Diseases,[‡] University of Connecticut School of Medicine, Farmington, Connecticut

Aminoacyl-tRNA synthetase-interacting multifunctional protein 1 (AIMP1; previously known as p43) is a multifunctional protein that was initially found in multitenzyme synthetase complex. In the present study, screening of the AIMP1-binding proteins revealed that AIMP1 can form a molecular complex with heat shock protein gp96. AIMP1 enhances gp96 dimerization and the interaction between gp96 and KDEL receptor-1 (KDEL-1), which mediates the retrieval of KDEL-containing proteins from Golgi to the endoplasmic reticulum (ER). The interaction between gp96 and KDEL-1 was reduced in AIMP1-deficient cells, and this disturbed ER retention of gp96 and increased its cell surface localization. Moreover, this localization of gp96 at the cell surface was suppressed by its interaction with AIMP1 and enhanced by the depletion of endogenous AIMP1. In addition, AIMP1-deficient mice showed dendritic cell activation attributable to increased gp96 surface presentation and lupus-like autoimmune phenotypes. These results suggest that AIMP1 acts as a regulator of the ER retention of gp96 and provide a new perspective of the regulatory mechanism underlying immune stimula-

tion by gp96. (Am J Pathol 2007, 170:2042–2054; DOI: 10.2353/ajpath.2007.061266)

AIMP1 (ARS-interacting multifunctional protein 1) was first reported as an auxiliary factor associated with macromolecular aminoacyl-tRNA synthetase (ARS) complex, which is composed of nine different enzymes and three nonenzyme factors, including AIMP1.¹ Among the complex-forming tRNA synthetases, AIMP1 binds and helps the catalytic reaction of arginyl-tRNA synthetase.² Recently, however, intracellular and extracellular noncanonical functions of complex-forming tRNA synthetases and nonenzyme factors have been reported.^{3,4} The noncanonical functions of AIMP1 mainly concern its extracellular functions on different target cells. AIMP1 shares partial homology with some inflammatory cytokines such as RANTES (regulated on activation, normal T cell expressed and presumably secreted) and MCP-1 (monocyte chemoattractant protein-1)⁵ and, in fact, acts as a cytokine on monocytes,^{6–8} endothelial cells,⁹ and fibroblasts,¹⁰ and has even been reported to act as a glucagon-like hormone.¹¹ AIMP1 has been detected in

Supported by the National Creative Research Initiatives of the Ministry of Science and Technology, Korea (to S.K.), the Korean Ministry of Science and Technology through the National Research Laboratory Program for Rheumatic Disease (to Y.W.S.), and the National Institutes of Health (grant no. CA100191 to Z.L.).

Accepted for publication February 23, 2007.

Supplemental material for this article can be found on <http://ajp.amjpathol.org>.

Address reprint requests to Sunghoon Kim, the National Creative Research Initiatives Center for Aminoacyl-tRNA Synthetase Network, College of Pharmacy, Seoul National University, Seoul 151-741, Korea; or Zihai Li, Center for Immunotherapy of Cancer and Infectious Diseases, University of Connecticut School of Medicine, 263 Farmington Ave., Farmington, CT 06030-1601. E-mail: sungkim@snu.ac.kr and zli@up.uconn.edu.

various unexpected cellular locations,¹² and AIMP1-deficient mice show diverse phenotypic disorders,^{10,11} which imply that it has additional physiological activities yet to be uncovered.

gp96 is the endoplasmic reticulum (ER)-resident member of the HSP90 family.¹³ Like other ER resident proteins, gp96 contains a C-terminal KDEL sequence, which is involved in retrograde transport from Golgi to the ER.¹⁴ However, despite this KDEL sequence, gp96 surface expression has been demonstrated on mouse Meth-A sarcoma cells but not on normal embryonic fibroblast cells.¹⁵ In addition, it has been reported that hsp species, including gp96, are expressed on murine thymocytes,¹⁶ which indicates that gp96 surface expression is not restricted to tumor cells.

Because gp96 has been implicated in innate and adaptive immunity,^{17,18} its surface expression may be of immunological relevance. gp96 has been implicated in the activation or maturation of dendritic cells (DCs).^{19–21} Direct interaction between gp96 and DCs via CD91 and TLR2/4^{22–24} induces DC maturation, and results in proinflammatory cytokine secretion and major histocompatibility class I and II up-regulation.^{24,25} Recently, transgenic mice expressing gp96 on cell surfaces were found to show significant DC activation and spontaneous lupus-like autoimmune disease development.²⁶ These results suggest that gp96 export from the ER is an important aspect of immune regulation and that the cell surface expression of gp96 must be tightly controlled to avoid unnecessary immune response.

The KDEL receptor is located at the Golgi and intermediate compartment^{27–29} and specifically binds KDEL-bearing proteins with high affinity in the Golgi³⁰ and then chaperones protein translocation to the ER, where the KDEL ligands are released. It has been proposed that the association between KDEL ligands and KDEL receptor in the Golgi occurs because this compartment has a lower pH than the ER and that, conversely, dissociation of KDEL ligand and KDEL receptor in the ER is favored by a relatively high pH.³¹ In this work, we suggest that AIMP1 acts to control gp96 retention by the ER and that disruption of interaction between these two molecules could initiate pathogenic pathways that lead to systemic autoimmune disease.

Materials and Methods

Mouse

AIMP1^{-/-} mice have been previously described in detail.^{10,11}

Antibodies, Chemicals, and Other Reagents

Most of the antibodies (Abs) used for flow cytometry were from BD Pharmingen (San Diego, CA). Mouse anti-c-Myc (9E10), mouse anti-glutathione S-transferase (GST), rabbit anti-gp96, rabbit anti-Fas, and mouse anti-tubulin antibodies were from Santa Cruz Biotechnology (Santa Cruz, CA). Mouse anti-KDEL receptor antibody was from Stressgen Biotechnologies, Inc. (San Diego, CA). Total

serum IgA, IgG1, IgG2a, IgG2b, IgG3, and IgM levels were determined using sandwich enzyme-linked immunosorbent assay (ELISA) kits from Southern Biotechnology Associates (Birmingham, AL). IgE level was determined by an ELISA kit from BD Biosciences (Mountain View, CA). Interferon- γ , interleukin (IL)-12 p40, IL-1 β , and tumor necrosis factor (TNF)- α levels were determined using specific ELISA kits from Pierce Biotechnology, Inc. (Rockford, IL). The 293, HL-60, and HeLa cell lines were purchased from the American Type Culture Collection (Manassas, VA).

Affinity Purification of AIMP1-Binding Proteins

Recombinant AIMP1 protein and bovine serum albumin (BSA) were biotinylated using sulfo-NHS-biotin reagent as instructed by the manufacturer (Pierce). Mouse pancreas was homogenized in homogenization buffer (25 mmol/L Tris, pH 7.4, 10 mmol/L NaCl, 0.5 mmol/L ethylenediaminetetraacetic acid, 0.5 mmol/L phenylmethyl sulfonyl fluoride, 1 μ g/ml leupeptin, 1 μ g/ml pepstatin A, and 5 μ g/ml aprotinin) containing 1% Triton X-100. Biotinylated AIMP1 and BSA preimmobilized streptavidin beads were incubated with 10 mg of protein extracts at 4°C for 12 hours. After washing, co-precipitated proteins were subjected to sodium dodecyl sulfate-polyacrylamide gel electrophoresis (SDS-PAGE). Major bands were excised and digested with trypsin (Roche Molecular Biochemicals, Indianapolis, IN) at 37°C for 6 hours, and the digested peptide fragment masses were determined using a Voyager DE time-of-flight mass spectrometer (Perceptiv Biosystems, Inc., Framingham, MA). Delayed ion extraction produced better than 50 ppm mass accuracies on average.

Coimmunoprecipitation

HL-60 cells or 293 cells, transfected with plasmid encoding AIMP1, were solubilized with lysis buffer (25 mmol/L Tris-HCl, pH 7.4, 10 mmol/L NaCl, 10% glycerol, 1 mmol/L ethylenediaminetetraacetic acid, 0.5% Triton X-100, 2 mmol/L dithiothreitol, and 1 mmol/L phenylmethyl sulfonyl fluoride, and aprotinin). Extracted proteins were mixed with anti-gp96 antibody (Santa Cruz) pre-coupled with protein A agarose and immunoblotted with anti-AIMP1 antibody.

In Vitro Binding Assay

Recombinant gp96 fragment proteins were expressed as GST fusion proteins and purified by glutathione Sepharose. The interaction between gp96 fragments and purified AIMP1 protein was tested using *in vitro* binding assays. Human gp96 wild type (WT) and E791 Δ were expressed as His (full length) or GST (amino acids 289 to 799) fusion proteins in *Escherichia coli*, and purified His-gp96 proteins were incubated with GST or GST-AIMP1. Purified GST-gp96 proteins were incubated with mock or AIMP1, and co-precipitation of gp96 and AIMP1 was determined by immunoblotting with anti-gp96 or anti-

AIMP1 antibody, respectively. Binding assay was conducted in 25 mmol/L Tris-HCl buffer (pH 7.4) containing 120 mmol/L NaCl, 10 mmol/L KCl, and 0.5% Triton X-100.

ELISA for Binding Assay

The pH-dependent binding of gp96 to AIMP1 was determined by ELISA. Briefly, 96-well plates (Maxisorp, F96; Nunc, Rochester, NY) were coated with 500 ng/well AIMP1 in phosphate-buffered saline (PBS) (pH 7.4). After washing, remaining sites were blocked with PBS containing 1% BSA for 1 hour. Binding of biotin-conjugated gp96 was performed in Tris buffer (25 mmol/L Tris, 10 mmol/L NaCl, and 0.4% Triton X-100) adjusted to pH 4, 5, 6, 7, 8, and 9. Plates were washed and incubated with horseradish peroxidase-conjugated streptavidin diluted in PBS, 0.1% BSA, and 0.1% Tween 20 for 30 minutes. The plates were washed, and then substrate was added to each well. The absorbance was monitored at 450 nm.

Flow Cytometry and Immunofluorescence Staining

After washing cells with $1 \times$ PBS, they were suspended in fluorescence-activated cell sorting (FACS) buffer ($1 \times$ PBS containing 2% fetal bovine serum, 1% BSA, and 0.1% sodium azide) and pretreated with the normal goat antibody. After washing, surface gp96 was monitored by flow cytometry using their respective antibodies. After staining, cells were washed and analyzed on a FACScan flow cytometer using CellQuest software (BD Biosciences). Surface gp96 on cultivated splenocytes was immunostained with anti-gp96 antibody and nuclear DNA with propidium iodide, and cells were observed under a confocal laser-scanning microscopy (μ -Radiance; Bio-Rad, Hercules, CA).

Subcellular Fractionation

Subcellular fractionation was performed as previously described.³²

Primary Cell Isolation and Culture

Spleens were isolated from 12-week-old AIMP1^{+/+} and AIMP1^{-/-} mice (C57BL/6), and cells were suspended in $1 \times$ PBS using a cell strainer (Becton Dickinson, Mountain View, CA), washed, and resuspended in $1 \times$ PBS. CD11c⁺ DCs were further enriched using a BSA density gradient. Thymocytes and splenocytes were isolated from 12-week-old mice and resuspended in RPMI 1640 media containing 10% fetal bovine serum, stained with appropriate Abs and subjected to flow cytometry.

Mixed Lymphocyte Reactions

Splenic DCs (8×10^3) were purified using CD11c magnetic beads (Miltenyi Biotec, Auburn, CA), fixed with 1% paraformaldehyde, and co-cultured with 1.5×10^5 puri-

fied allogeneic CD4⁺ T cells. Fifty-six hours later, cells were pulsed with 1 μ Ci of [³H]thymidine, and ³H incorporation was determined using a liquid scintillation counter.

Autoimmune Test

Lung and liver tissue sections of AIMP1^{+/+} and AIMP1^{-/-} mice were fixed in 10% formaldehyde in PBS and dehydrated using an alcohol gradient. After paraffin infiltration, tissues were sectioned using a microtome, hematoxylin and eosin (H&E)-stained, and analyzed by light microscopy. To determine the presence of autoantibodies reacting with their self-nuclear antigens, serum was separated from mouse blood using a clot activator (Becton Dickinson) and used for immunoblotting nuclear proteins extracted from autologous liver tissues. Anti-nuclear antibodies (ANAs) were also measured in serum by indirect immunofluorescence using HEP-2-coated slides (INOVA Diagnostics, Inc., San Diego, CA). Slides were first incubated with 1:40 diluted mouse serum in PBS for 30 minutes. After washing with PBS, fluorescein isothiocyanate (FITC)-labeled goat anti-whole mouse Ig (BD Biosciences) was added for 30 minutes. All stages were performed in a dark, humidified chamber at room temperature. Slides were then washed, mounted using mounting medium (Biomed, Foster City, CA), and viewed under a fluorescence microscope. Kidneys from AIMP1^{+/+} and AIMP1^{-/-} mice were sectioned using a cryostat. These cryosections were blocked with normal goat serum and then stained with FITC-conjugated goat anti-mouse Ig. Nuclear DNA was stained with propidium iodide and observed under a confocal laser-scanning microscope.

DC Maturation Assay

Bone marrow-derived immature DCs (1×10^4) from WT mice were stimulated with fixed, DC-depleted splenocytes (2×10^5) from WT or AIMP1^{-/-} mice for 16 hours. DCs were stained with Abs against CD83 and CD86 and subjected to FACS analysis. Culture supernatants were collected for cytokine assays using ELISA kits from Pierce Biotechnology Inc.

Bone Marrow Transplantation

Bone marrow cells (2×10^6) were injected via a tail vein into WT mice that had been previously lethally irradiated (550×2 Gy with an interval of 4 hours) 24 hours before transfer.

Transfection of Small Interfering RNAs (siRNAs)

Endogenous AIMP1 or gp96 were depleted using standard siRNA techniques. Briefly, cells were seeded into six-well plates and, when 50% confluent, transfected with siRNA duplexes (final concentration, 50 nmol/L) (Invitro-

gen, Carlsbad, CA) using Lipofectamine 2000 (Invitrogen) according to the manufacturer's instructions. The greatest decreases in endogenous AIMP1 and gp96 occurred at 48 hours after transfection without affecting cell viability. All siRNAs were 25-nucleotide duplexes and had the following sequences: AIMP1, 5'-GGAGCUGAAUCCUAAGAAGAAGAUU-3'; gp96-411, 5'-UUAUCUUGUCUAAAG CAUCAGAAGC-3'; gp96-749, 5'-AUUGGAGUCUGAUUCCCAGAUGUGC-3'; and gp96-895, 5'-AAGUUGAUGAACUGAGAGU ACUUC-3'.

Statistical Analysis

The Student's *t*-test was used for statistical analysis. *P* values of <0.05 were considered to represent statistically significant differences.

Results

Identification of gp96 as an AIMP1 Binding Protein

Recent reports show that the components of ARS complex participate in various biological processes in addition to protein synthesis.³³⁻⁴⁰ To explore the novel activities of AIMP1, we performed affinity purification to search for cellular proteins that associate with AIMP1. Proteins co-purified with AIMP1 were identified by mass spectrometry. The bound proteins were determined to be gp96 and a few tRNA synthetases, which are known to form a complex with the AIMP1⁴ and COPI complex subunits involved in ER/Golgi transport (Figure 1A). The interaction between AIMP1 and gp96 or β -COP, a component of COPI complex, was further determined by Western blotting (Figure 1B). Recombinant gp96 was also co-purified with GST-fused AIMP1 (Figure 1C), suggesting direct binding of AIMP1 with gp96. AIMP1 was coimmunoprecipitated with gp96 (Figure 1D). To further investigate the interaction between AIMP1 and gp96, the binding of gp96 to recombinant AIMP1 was examined using ELISA. gp96 was found to bind to AIMP1 in a dose-dependent manner, and this binding was saturable (Figure 1E) with a dissociation constant (k_d) of gp96 to AIMP1 of 0.117 ± 0.003 nmol/L. Moreover, the interaction between AIMP1 and gp96 was found to be pH-dependent, with maximal binding at pH 5 (Figure 1F).

To identify the interaction regions involved in this interaction, we expressed a variety of deletion mutants of AIMP1⁴¹ or gp96 and performed an *in vitro* binding assay. It was found that the AIMP1 domain spanning amino acids 54 to 192 interacts with gp96, indicating that AIMP1 uses different domains for binding to gp96 and arginyl-tRNA synthetase (RRS) (Figure 1G). In addition, it was found that its interactions with these two different targets can occur independently (Supplementary Figure 1 at <http://ajp.amjpathol.org>). These results indicate that gp96 interacts with AIMP1 independently of tRNA synthetase complex.

gp96 can be divided into a number of functional domains. The peptide region from 22 to 287 is responsible

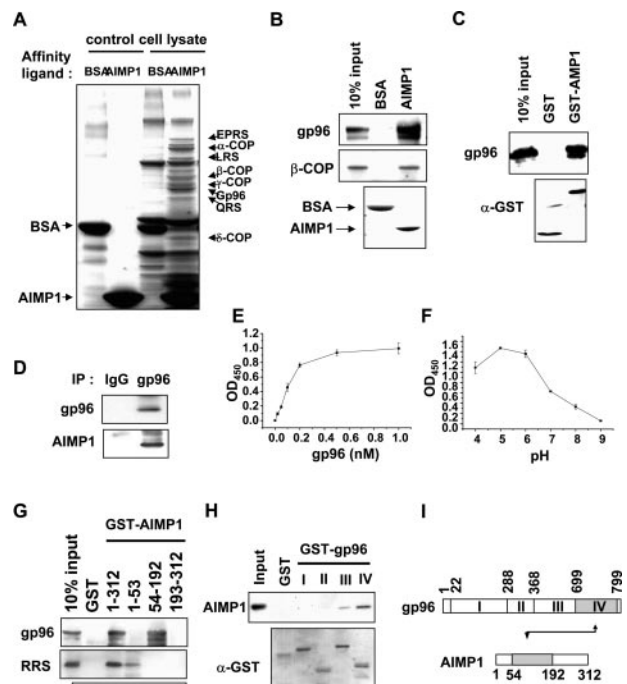


Figure 1. Identification of gp96 as an AIMP1 binding protein. **A:** The protein extracts from mouse pancreas were purified with biotinylated BSA or AIMP1, separated by SDS-PAGE, and then visualized by silver staining plus (Bio-Rad). **Arrows** indicate AIMP1-binding proteins. **B:** Protein extracts from mouse pancreas were purified with biotinylated BSA or AIMP1, separated by SDS-PAGE, and then immunoblotted with anti-gp96 or β -COP antibody. Inputs are the amounts of pancreatic protein extract used. **C:** Protein extracts from mouse pancreas were purified with GST or GST-AIMP1, separated by SDS-PAGE, and then immunoblotted with anti-gp96 or GST antibody. Inputs are the amounts of pancreatic protein extract used. **D:** Proteins extracted from HeLa cells were immunoprecipitated with anti-gp96 antibody or a control IgG, and precipitated proteins were immunoblotted with anti-gp96 and anti-AIMP1 antibody. **E:** Interactions between AIMP1 and gp96 were determined by ELISA. Biotin-conjugated gp96 was added to microtiter wells coated with AIMP1 at pH 7.4, and bound gp96 was detected with peroxidase-conjugated streptavidin. **F:** The pH dependency of interaction between AIMP1 and gp96 was determined by ELISA. Biotin-conjugated gp96 was added to microtiter wells coated with AIMP1 in various pH buffers (pH 4, 5, 6, 7, 8, and 9). Bound gp96 was detected with peroxidase-conjugated streptavidin. **G:** The 312-amino acid full-length (AIMP1-F), 1- to 53-amino acid, 54- to 192-amino acid, and 193- to 312-amino acid peptides were expressed as GST fusion proteins in *E. coli*, and their expressions were confirmed by Ponceau staining. Purified GST-AIMP1 fragments were incubated with HeLa cell lysates and the co-precipitation of gp96 and RRS was determined by immunoblotting with anti-gp96 or RRS antibodies. Inputs are the amounts of HeLa cell protein extract used. **H:** Each of the functional domains of gp96 was expressed as GST fusion protein in *E. coli*. Purified GST-gp96 fragments were incubated with AIMP1, and the co-precipitation of AIMP1 was determined by immunoblotting with anti-AIMP1 antibody. Inputs are the amounts of purified AIMP1 protein used. **I:** The functional domains of AIMP1 and gp96 are schematically represented. The interaction between the two involves 54 to 192 of AIMP1 and the C-terminal dimerization domain of gp96. The data shown are representative of three separate experiments.

for nucleotide/geldanamycin binding, and the region from 288 to 368 is an acidic domain.¹³ In addition, the region from 697 to 799 is involved in gp96 oligomerization and self-assembly.⁴ We expressed each of these functional domains as GST fusion proteins and precipitated them with glutathione Sepharose. AIMP1 co-precipitated with the dimerization domain of gp96, but it also showed a weak affinity for domain III (Figure 1H). Combined

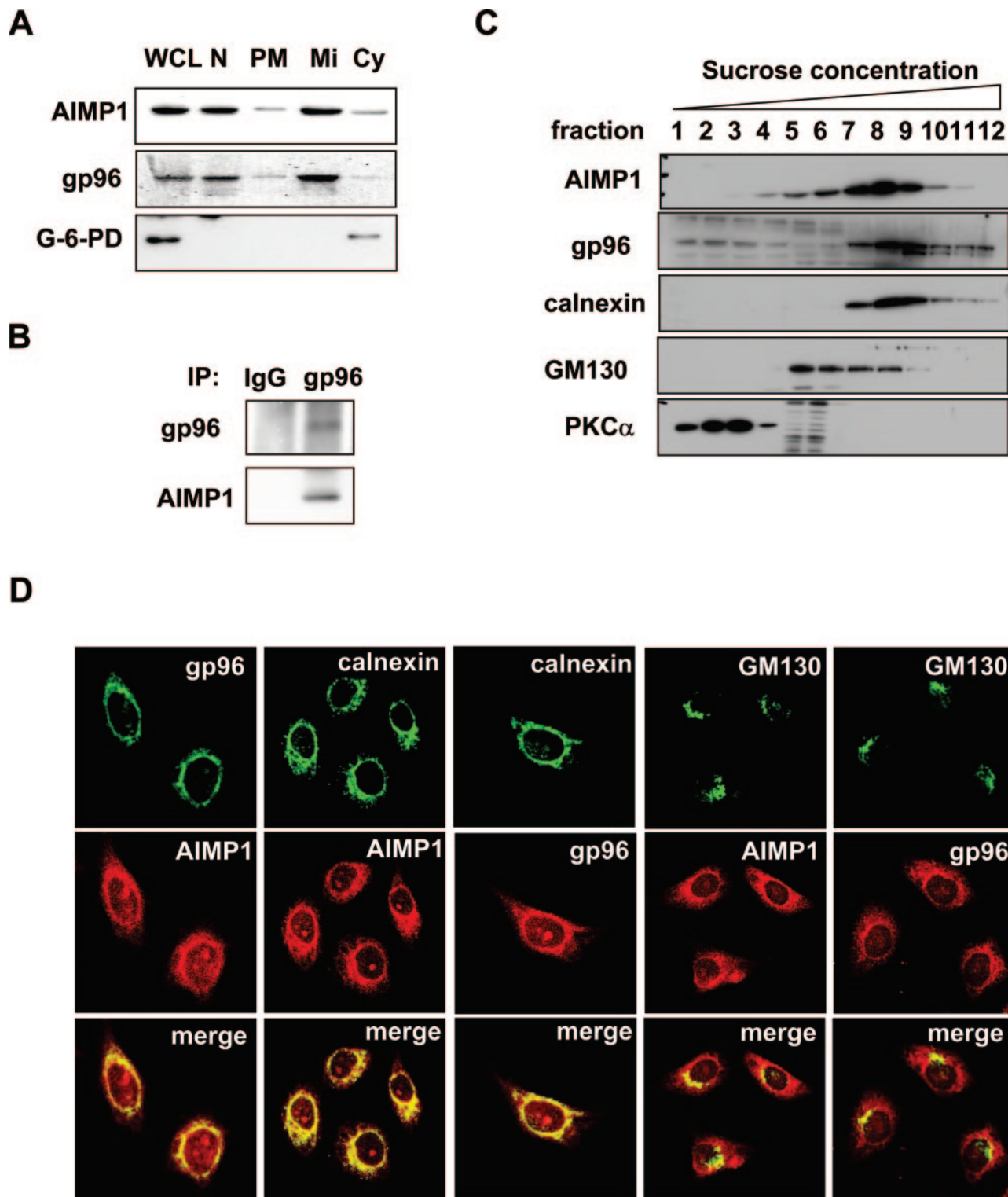


Figure 2. Subcellular localization of AIMP1 and gp96. **A:** Subcellular fractionation of AIMP1 and gp96. Fifty μ l of each subcellular fraction was subjected to immunoblotting with anti-AIMP1 and gp96. G-6-PD (glucose-6-phosphate dehydrogenase) was used as a cytosol marker. WCL, whole cell lysates; N, nucleus; PM, plasma membrane; Mi, microsome; Cy, cytosol. **B:** Proteins extracted from the microsomal fraction were immunoprecipitated with mock IgG or anti-gp96 antibody. The coimmunoprecipitation of AIMP1 was determined by immunoblotting with anti-AIMP1 antibody. **C:** Sucrose gradient fractionation of membranes. Supernatant ($1000 \times g$) of HeLa cell homogenate was layered onto a discontinuous sucrose gradient. After centrifugation, 12 fractions were collected from the top of the tube, and 50 μ l of each fraction were immunoblotted with anti-AIMP1 and gp96. Calnexin was used as an ER marker, GM130 as a Golgi marker, and PKC α as a cytosol marker. **D:** Immunofluorescence staining of AIMP1 and gp96 in HeLa cells. HeLa cells were reacted with anti-AIMP1, anti-gp96, anti-calnexin (ER marker), or anti-GM130 (Golgi marker) antibodies and visualized with FITC-conjugated (green) and tetramethylrhodamine B isothiocyanate-conjugated (red) secondary antibodies, respectively. Data shown are representative of three independent experiments.

together, the results indicate that the peptide region from 54 to 192 of AIMP1 interacts with the C-terminal amino acids 699 to 799 region of gp96 (Figure 1I).

gp96 seems to form a deletion variant at E791 (E791Δ), because this variant is included in GenBank and has been validated by multiple, independent refSNP cluster submissions. Thus, we examined whether the E791Δ variant has a different affinity for AIMP1 compared with wild-type (WT) gp96 using an *in vitro* pull-down assay. The WT and the gp96 deletion variant both fused to GST and incubated with purified AIMP1 for affinity precipitation (Supplementary Figure 2A at <http://ajp.amjpathol.org>). In addition, GST or GST-fused AIMP1 were incubated with purified WT or gp96 deletion variant, and the co-precipitations of these proteins were determined (Supplementary Figure 2B at <http://ajp.amjpathol.org>). In both assays, the E791Δ variant showed severely reduced affinity for AIMP1 as compared with the WT protein, indicating that the C-terminal glutamic acid-rich sequences near the KDEL motif of gp96 are important for AIMP1 binding.

Next, we examined the subcellular localization of the interaction between AIMP1 and gp96. Cell fractionation analysis revealed co-fractionation of AIMP1 with gp96 within the microsomal fraction (Figure 2A), and AIMP1 also co-precipitated with gp96 from this fraction (Figure 2B). Sucrose density gradient analysis further separated the microsomal fraction into ER and Golgi-enriched fractions (Figure 2C), and both AIMP1 and gp96 co-fractionated with the ER marker, calnexin, and minor amounts co-fractionated with the Golgi marker GM130. Furthermore, AIMP1 and gp96 were well co-localized with calnexin except for a minor amounts of nuclear AIMP1 and of AIMP1 co-localized with gp96 and GM130 (Figure 2D).

Significance of AIMP1 in the Dimerization of gp96 and in the Interaction between gp96 and KDELR-1

The HSP90 family proteins studied to date are known to exist as dimers,^{42,43} and AIMP1 is also known to be a dimer^{44,45} and to interact with the C-terminal dimerization domain of gp96 (Figure 1H). Therefore, we investigated whether AIMP1 can regulate gp96 dimer formation. Overexpression of AIMP1 increased the amount of His-tagged gp96 coimmunoprecipitated with GFP-tagged gp96 (Figure 3, A and B).

KDEL receptor mediates the retrieval of escaped ER proteins bearing the KDEL or HDEL signal.²⁸ This occurs throughout retrograde trafficking mediated by COPI-coated transport carriers.⁴⁶ Because the COPI components, coatamer subunit α , β , γ , and δ associated with AIMP1 (Figure 1A), we considered that AIMP1 might play a role in the retrieval of gp96 from Golgi to the ER by forming a complex with KDEL receptor and COPI components, and thus, we examined the complex formation of AIMP1 with KDELR-1. It was found that the recombinant 54 to 192 amino acids fragment of AIMP1, which is a binding site for gp96 (Figure 1G), also precipitated KDELR-1 (Supplementary Figure 3 at <http://ajp.amjpathol.org>). We then analyzed the interaction between

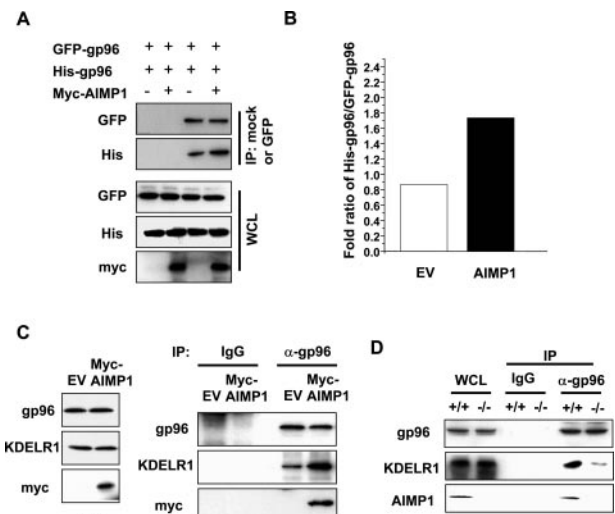


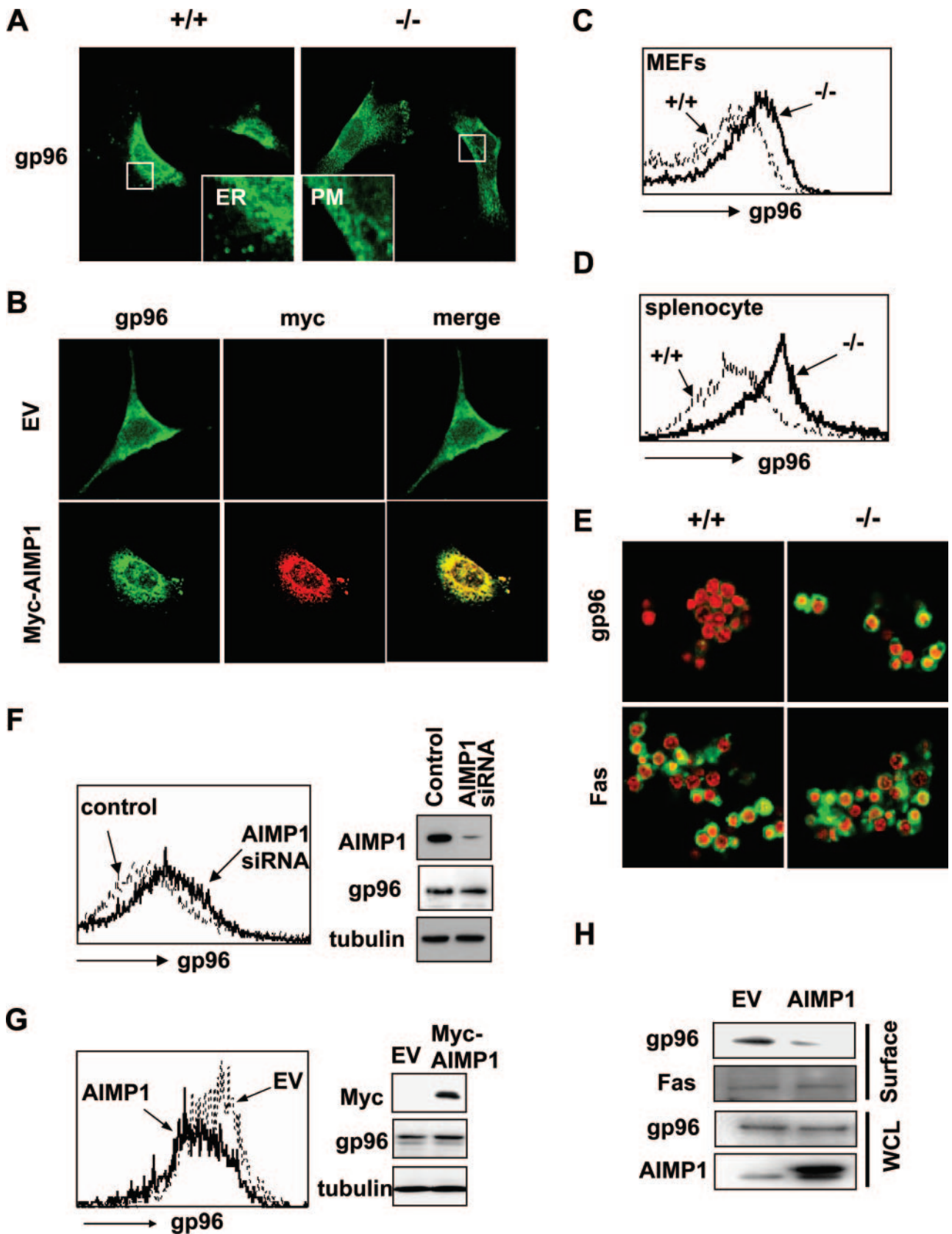
Figure 3. Functional significance of AIMP1 for gp96 dimerization and complex formation between gp96 and KDELR-1. **A:** Proteins extracted from GFP-tagged gp96, His-tagged gp96, and myc-tagged AIMP1-transfected 293 cells were immunoprecipitated with control IgG or anti-GFP antibody, and precipitated proteins were immunoblotted using anti-His antibody. WCL, whole cell lysates. **B:** Fold ratios of His-tagged gp96 bound to GFP-tagged gp96 from **A** were quantified by densitometry. **C:** Left: The expressions of gp96, KDELR-1, and myc-AIMP1 were determined by Western blotting. Right: Proteins extracted from control vector or myc-tagged AIMP1-transfected 293 cells were immunoprecipitated using anti-gp96 antibody, and the precipitated proteins were immunoblotted using anti-KDELR-1 or anti-myc antibodies. **D:** Proteins extracted from WT or AIMP1^{-/-} MEFs were immunoprecipitated using anti-gp96 antibody or a control IgG, and precipitated proteins were immunoblotted using anti-gp96, anti-AIMP1, and anti-KDELR-1 antibodies. Data shown are representative of three independent experiments.

gp96 and KDELR-1 in AIMP1-overexpressed cells and AIMP1^{+/+} or AIMP1^{-/-} cells and found that gp96 forms a complex with AIMP1 and KDELR-1 (Figure 3, C and D) and that the association between gp96 and KDELR-1 was elevated in AIMP1-overexpressing cells (Figure 3C) and attenuated in the absence of AIMP1 (Figure 3D), which implies that AIMP1 assists in the anchoring of gp96 to KDELR-1 to facilitate the ER retention of gp96.

Significance of AIMP1 in the Subcellular Localization of gp96

Next, we examined the subcellular localizations of gp96 in AIMP1^{+/+} or AIMP1^{-/-} mouse embryonic fibroblast (MEF) cells. gp96 was found to be mainly localized to perinuclear ER in WT MEFs, as previously described, but was dispersed from the ER and localized to the plasma membrane in AIMP1^{-/-} MEFs (Figure 4A). Furthermore, the overexpression of AIMP1 in AIMP1^{-/-} MEFs relocated gp96 to the ER, thus suggesting that the ER retention of gp96 is regulated by AIMP1 (Figure 4B).

The location of gp96 after release from the ER remains somewhat controversial. Based on previous reports, there are two possibilities for gp96 localization: the extracellular secretion of gp96^{47,48} and its cell surface presentation.^{21,49,50} In this study, we analyzed the culture media of WT and AIMP1^{-/-} MEFs for the presence of gp96 but failed to detect it (data not shown). However, gp96 was detected on cell surfaces by FACS (Figure 4C). Moreover, AIMP1^{-/-} splenocytes had higher gp96 cell



surface expressions than WT cells (Figure 4, D and E), whereas no differences were observed on the surface level of Fas by immunofluorescence microscopy (Figure 4E). This higher cell surface localization of gp96 was observed not only in AIMP1^{-/-} splenocytes but also in a variety of AIMP1^{-/-} cells in the bone marrow-derived Gr-1⁺, CD11b⁺, and B220⁺ cell populations (Supplementary Figure 4 at <http://ajp.amjpathol.org>). When endogenous AIMP1 was suppressed using its specific siRNA in HeLa cells, gp96 surface levels were enhanced (Figure 4F). In contrast, the overexpression of AIMP1 in 293 cells substantially reduced gp96 surface levels, as determined by flow cytometry (Figure 4G) and by surface biotinylation (Figure 4H) without changing the total cellular level of gp96. Based on these observations, AIMP1 seems to regulate the KDELR-1-mediated ER retention of gp96, and AIMP1 deficiencies result in gp96 movement to the plasma membrane. Whether gp96 is retained in the plasma membrane or eventually released to the extracellular matrix requires further investigation.

Activation of DCs in AIMP1-Deficient Mice

gp96 has been implicated in the activation and maturation of DCs via CD91 and Toll-like receptor (TLR) 2/4.²²⁻²⁵ We next investigated whether DCs are activated in AIMP1^{-/-} mice, as suggested by the above experiments. Eight-week-old AIMP1^{-/-} mice contained more CD4⁺ DCs than the WT (20.45 versus 11.14%) (Figure 5A), suggesting a change of DC subset and the induction of Th2 responses.^{51,52} Of the known DC maturation markers, ICOSL (ligand for inducible co-stimulatory molecule) showed the most prominent increase in AIMP1^{-/-} cells versus the WT (53.66 versus 18.14%) (Figure 5, B and C). CD80 and OX40 ligand (OX40L) were slightly elevated in the absence of AIMP1 (93.23 versus 90.29% and 5.24 versus 3.97%, respectively), whereas other maturation markers, such as CD83 and MHC class II were similarly expressed in AIMP1^{-/-} CD11c(high) DCs (Supplementary Figure 5 at <http://ajp.amjpathol.org>). The increased expression of cell surface ICOSL correlates well with the increased ability of AIMP1^{-/-} splenic DCs to activate allogeneic naïve WT or AIMP1^{-/-} CD4⁺ T cells, as measured by proliferation (Figure 5D) and secretion of TNF- α (Figure 5E) and interferon- γ (Figure 5F). Based on these immunological characteristics, we conclude that DCs in AIMP1^{-/-} mice are hyperfunctional in stimulating T cells.

The Effect of Increased Cell Surface gp96 on DC Activation

To determine the importance of surface gp96 in the activation of DCs in AIMP1^{-/-} mice, we silenced gp96 expression with its siRNA and examined its effect on DC activation. It was found that the transfection of splenocytes with siRNA corresponding to nucleotides 895 to 915 of mouse gp96 mRNA (designated 895) reduced both total (Figure 6A) and surface gp96 levels (Figure 6B). A DC maturation experiment was then performed by co-culturing WT bone marrow-derived DCs (BMDCs) with DC-depleted WT or AIMP1^{-/-} splenocytes, pretreated with 895 or control siRNA. It was found that AIMP1^{-/-} splenocytes matured DCs more efficiently than WT splenocytes, as evidenced by the up-regulations of CD83 and CD86 (Figure 6, C and D) and by the productions of IL-12 p40, IL-1 β , and TNF- α (Figure 6, E-G). However, the reduction of cell surface gp96 in AIMP1^{-/-} splenocytes by siRNA prevented DC maturation (Figure 6, C-G).

gp96-defective mutant cell lines were previously shown to be unresponsive to bacterial components because of the intracellular retention of TLRs.⁵³ To determine whether the effect shown here was because of the suppression of surface molecules like TLR4, we compared the surface TLR4 levels of control and gp96 siRNA-transfected splenocytes by flow cytometry, but no difference was found between the two (data not shown), which excludes the possibility that the effects of gp96 siRNA on DC activation are the result of changes in the expression of surface molecules other than gp96. These data suggest that the increased DC maturation shown by AIMP1^{-/-} cells is primarily the result of increased gp96 surface expression.

AIMP1-Deficient Mice Develop Lupus-Like Autoimmune Phenotypes

DCs play critical roles in the maintenance of immunological tolerance⁵⁴⁻⁵⁶ and in the pathogenesis of autoimmunity.^{57,58} In addition, chronic maturation of tissue DCs can induce severe organ-specific autoimmune disease and systemic autoimmunity.⁵⁹ To determine the relationship between hyperactive DCs and *in vivo* phenotypes, we undertook systemic histological examinations in

Figure 4. Functional significance of the interaction between AIMP1 and gp96 in terms of the subcellular localization of gp96. **A:** Immunofluorescence staining of gp96 in WT or AIMP1^{-/-} MEFs. gp96 was visualized using secondary antibody conjugated with FITC. ER and PM mean endoplasmic reticulum and plasma membrane, respectively. **B:** Immunofluorescence staining of myc-AIMP1 and gp96 in AIMP1^{-/-} MEFs. AIMP1^{-/-} MEFs were transfected with EV (empty vector) or myc-tagged AIMP1, and then cells were reacted with anti-gp96 or anti-myc antibodies and visualized with FITC-conjugated (green) and TRITC-conjugated (red) secondary antibodies, respectively. **C:** MEFs from AIMP1^{+/+} (dotted line) and AIMP1^{-/-} (solid line) mice were stained for cell surface gp96, followed by flow cytometry analysis. **D:** Splenocytes from AIMP1^{+/+} (dotted line) and AIMP1^{-/-} (solid line) mice were stained for cell surface gp96, followed by flow cytometry analysis. **E:** Surface gp96 in splenocytes isolated from AIMP1^{+/+} and AIMP1^{-/-} mice were subjected to immunofluorescence staining with polyclonal anti-gp96 or anti-Fas antibody (green) and nuclei were stained with propidium iodide (red). At least three mice per group were examined. Fas was used as a surface marker. Surface gp96 staining was also observed using monoclonal anti-gp96 antibody and titrated by the addition of exogenous recombinant gp96 (data not shown). **F:** Left: HeLa cells were transfected with control (dotted line) or AIMP1 siRNA (solid line) for 48 hours, and surface gp96 expression was determined by flow cytometry. Right: The effect of siRNA on AIMP1 expression was determined by Western blotting. **G:** Left: The effect of AIMP1 on the surface expression of gp96 was determined by flow cytometry in 293 cells after transfection of empty vector (EV) and AIMP1. Right: The effect of AIMP1 on the total cellular level of gp96 was determined by Western blotting with the corresponding antibodies. Tubulin was used as a loading control. **H:** The surface proteins of 293 cells transfected with EV or AIMP1 were biotinylated with sulfo-NHS-biotin and precipitated using streptavidin beads. Total cellular proteins (WCL) and precipitated proteins (surface) were immunoblotted with anti-gp96, anti-Fas, and anti-AIMP1 antibodies. Data shown are representative of three independent experiments.

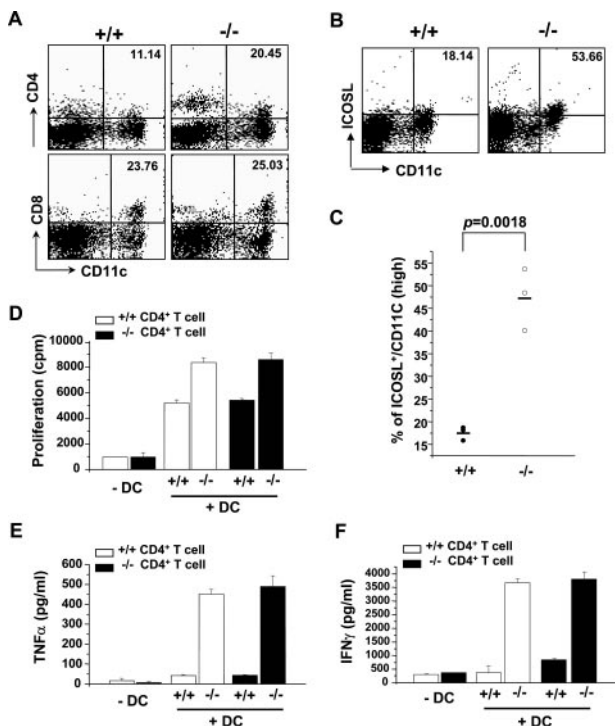


Figure 5. Activation of DCs in AIMP1-deficient mice. **A:** Splenic CD11c⁺ cells from AIMP1^{+/+} or AIMP1^{-/-} mice ($n = 3$) were analyzed by flow cytometry for the expression of CD4 ($P < 0.05$) and CD8 ($P > 0.05$). Percentages of CD4⁺/CD11c⁺ cells or CD8⁺/CD11c⁺ cells are indicated. **B:** Splenic CD11c⁺ cells from AIMP1^{+/+} or AIMP1^{-/-} mice ($n = 3$) were analyzed by flow cytometry for ICOSL expression on cell surfaces. Representative data from one mouse per group are shown, and the percentages of maturation marker⁺/CD11c⁺(high) cells are indicated. **C:** Splenic CD11c⁺ cells from AIMP1^{+/+} or AIMP1^{-/-} mice ($n = 3$) were analyzed by flow cytometry for surface ICOSL expression ($P = 0.0018$). **D:** Freshly isolated CD11c⁺ splenic DCs from WT or AIMP1^{-/-} mice were tested for their abilities to stimulate allogeneic naïve WT or AIMP1^{-/-} CD4⁺ T cells to proliferate by [³H]thymidine incorporation ($P < 0.01$) and for their abilities to produce TNF- α ($P < 0.01$) (**E**) and interferon- γ ($P < 0.01$) (**F**) by ELISA. Data represent the mean \pm SD.

AIMP1^{-/-} mice. One of the most prominent phenotypes was that most female AIMP1^{-/-} mice developed systemic inflammatory cell infiltration of organs, such as lung and liver, at 12 weeks of age (Figure 7A). Further examination of these mutant mice revealed various signatures of autoimmunity. For example, the nuclear proteins of AIMP1^{-/-} mice reacted to antibodies in their own sera from 9 weeks, demonstrating the onset of autoantibody production (Figure 7B). In addition, immunofluorescence analysis revealed ANAs in the sera of AIMP1^{-/-} mice and depositions of immune complexes in the glomeruli of the kidneys of AIMP1^{-/-} mice, as evidenced by the presence of mouse IgG (Figure 7C). Mutant mice also showed significant hypergammaglobulinemia, as evidenced by the increase of IgG1, IgG2a, IgM, and IgE (Figure 7D). Based on these phenotypes, we concluded that AIMP1 deficiency leads to the development of systemic lupus-like autoimmune diseases. To exclude the involvement of thymic environment in these phenotypes, we performed a bone marrow chimera experiment, by reconstituting 6-week-old irradiated WT mice with AIMP1^{-/-} bone marrow. Six months later, we found that AIMP1^{-/-}→WT mice developed both ANA (Figure 7E) and glomerulonephritis

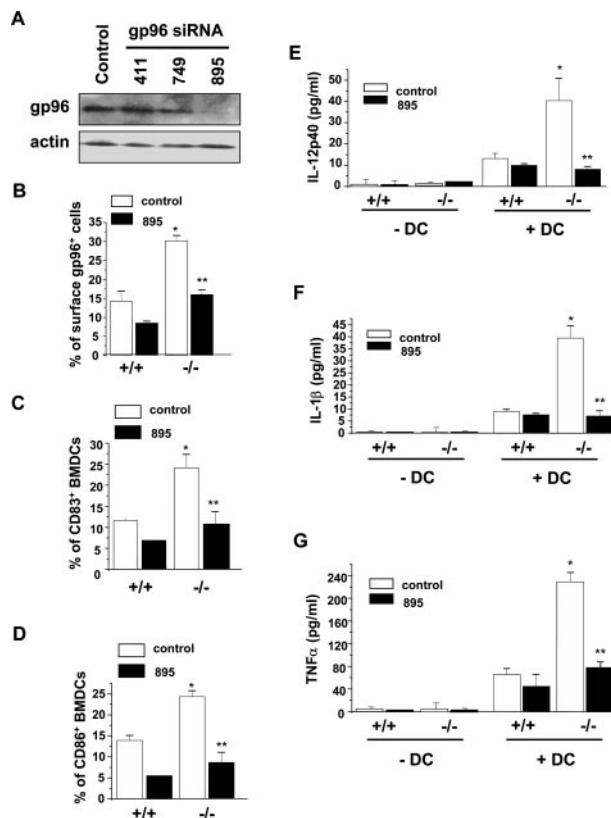


Figure 6. The effect of increased cell surface gp96 in AIMP1^{-/-} cells on DC activation. **A:** CD11c⁺ DC-deprived WT splenocytes were transfected with control or gp96 siRNA for 48 hours, and gp96 expressions were determined by immunoblotting. **B:** CD11c⁺ DC-deprived WT or AIMP1^{-/-} splenocytes were transfected with control or gp96 siRNA for 48 hours, and surface gp96 was determined by flow cytometry. ($*P < 0.01$, $**P < 0.01$). CD11c⁺ DC-deprived splenocytes (2×10^5 cells) from WT or AIMP1^{-/-} mice were transfected with control or gp96 siRNA and then co-cultured with WT BMDCs (1×10^4 cells) for 16 hours. WT BMDCs were then analyzed by FACS for CD83 ($*P < 0.01$, $**P < 0.01$) (**C**) and CD86 cell surface expression ($*P < 0.01$, $**P < 0.01$) (**D**) or by ELISA to determine the release of IL-12p40 ($*P < 0.01$, $**P < 0.01$) (**E**), IL-1 β ($*P < 0.01$, $**P < 0.01$) (**F**), and TNF- α ($*P < 0.01$, $**P < 0.01$) (**G**) by WT BMDCs. Data represent the mean \pm SD.

(Figure 7F), whereas no autoimmunity was evident in AIMP1^{+/+}→WT chimeras, thus demonstrating that the autoimmune phenotype associated with AIMP1^{-/-} mice is hematopoietic system autonomous.

To gain insight into the pathological basis of the autoimmune phenomenon associated with AIMP1 ablation, we performed a systemic immunophenotypical analysis on the hematopoietic system of AIMP1^{-/-} mice. No alterations were found in the distributions of major subsets of thymic and splenic T cells (CD4⁻CD8⁻, CD4⁺, CD8⁺, CD4⁺CD8⁺) from 12 weeks of age in WT or AIMP1^{-/-} mice (Supplementary Figure 6A at <http://ajp.amjpathol.org>). In addition, no alterations were observed in the distribution of CD44⁺, memory/activated T-cell marker, subsets of thymic CD4⁺ T cells (Supplementary Figure 6B at <http://ajp.amjpathol.org>). In addition, we analyzed regulatory T cells, because they are also known to play critical roles in the maintenance of immunological tolerance. However, no differences between WT and AIMP1^{-/-} mice with respect to the frequencies of thymic and splenic CD4⁺CD25⁺ or CD8⁺CD25⁺ regulatory T

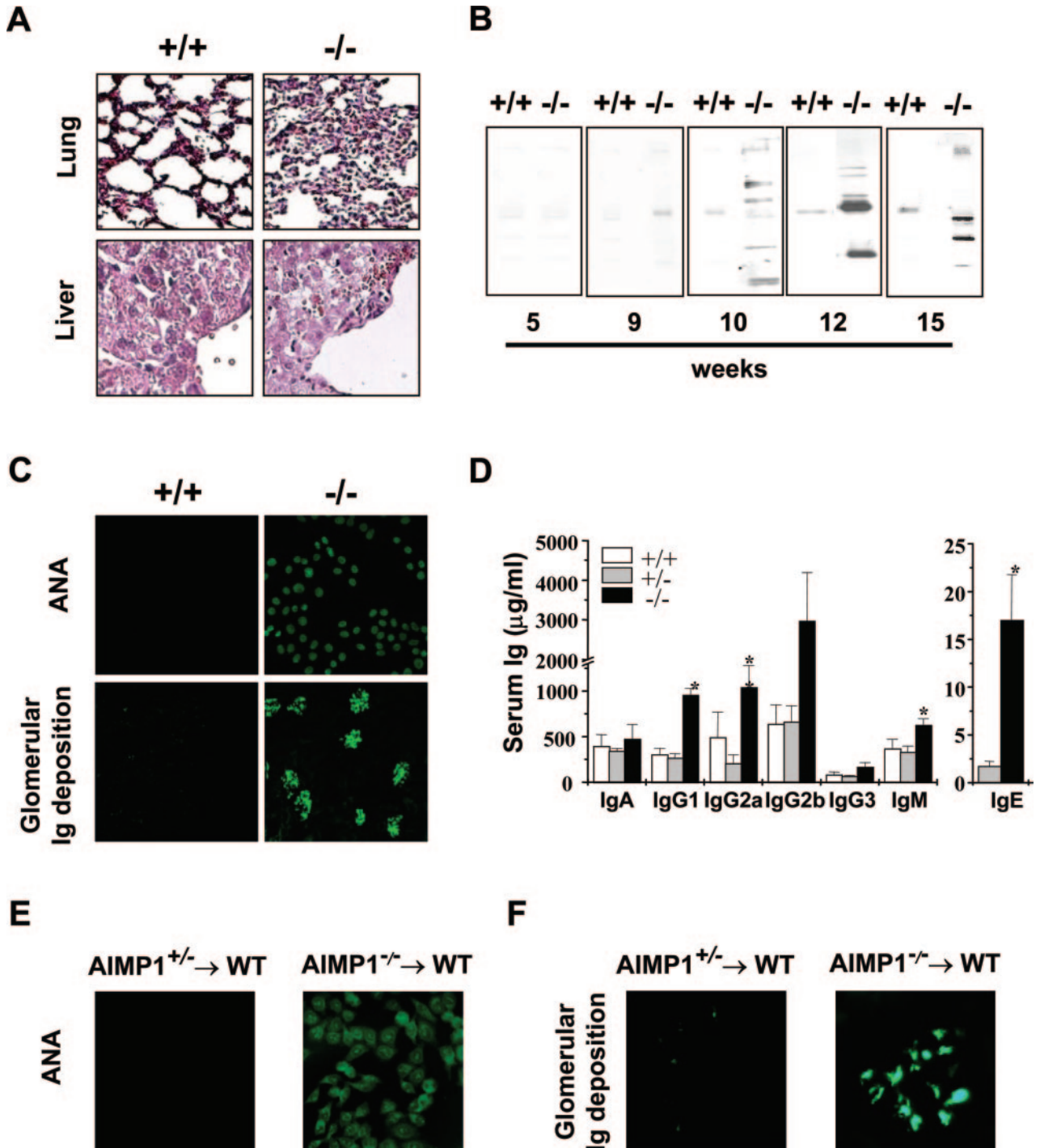


Figure 7. AIMP1-deficient mice develop systemic lupus-like autoimmune diseases. **A:** Five- μ m lung and liver tissue sections of AIMP1^{+/+} and AIMP1^{-/-} mice were stained with H&E. **B:** Nuclei were isolated from livers of AIMP1^{+/+} and AIMP1^{-/-} mice at the indicated ages, and nuclear proteins separated by SDS-PAGE were immunoblotted with autologous sera. **C:** Top: Immunofluorescence assay for the presence of ANA. At least four mice per group were examined. Bottom: Kidney sections were analyzed by immunofluorescence microscopy after staining with antibody against mouse IgG (green). Data from one representative mouse are shown. **D:** Serum Ig levels from age-matched WT ($n = 5$), AIMP1^{-/-} ($n = 5$), and AIMP1^{+/-} ($n = 4$) littermates by ELISA. * $P < 0.001$, ** $P < 0.05$ (WT versus AIMP1^{-/-}). Data represent the mean \pm SD. **E:** WT mice were lethally irradiated (550 cGy \times 2) and then transplanted intravenously with bone marrow from AIMP1^{-/-} mice or AIMP1^{+/-} littermates. Six months after transplantation, sera were collected from recipient mice and tested for the presence of ANA (**E**) and glomerular Ig deposition (**F**) as described above. Data from one representative mouse per group ($n = 3$) are shown. Original magnifications, $\times 100$ (**A**).

cells were observed before age 12 weeks (data not shown). We also confirmed that the development of regulatory T cells at 11 weeks in WT or AIMP1^{-/-} mice was unaltered, by examining the expression of Foxp3, a reg-

ulatory T-cell-specific transcription factor,⁶⁰ in WT and AIMP1^{-/-} thymic CD4⁺ T cells (Supplementary Figure 6, C and D, at <http://ajp.amjpathol.org>). Furthermore, AIMP1 deficiency was not found to affect overall protein synthe-

sis in thymic epithelial cells (data not shown), which argues against the possibility of impaired negative selection as result of inefficient antigen expression in the thymus.

Discussion

This study demonstrates that the interaction between AIMP1 and gp96 as an important component of a mechanism that controls immunological tolerance. The immunological properties of extracellular gp96 have been previously illustrated by genetic manipulation, and these studies confirm its constitutive extracellular exposure.^{47,48,61} Our finding that AIMP1 is a natural regulator of gp96 surface export has both immunological and cellular implications. It has been suggested that HSPs are endogenous danger molecules that trigger productive immune responses during bacterial or viral infections or after mechanical injury. During the normal steady state, the proinflammatory properties of HSPs are tightly regulated to avoid unnecessary immune response. Thus, the control of KDEL receptor-mediated gp96 retrieval by AIMP1 might represent an important switch for the regulation of immunity and the tolerance of adaptive immunity.

Although AIMP1 was first reported as a factor associated with the multitRNA synthetase complex, it was also identified as cytokine in the extracellular matrix^{6,8-10} and was even found to be secreted to blood as a glucagon-like hormone.¹¹ Thus, it is not surprising that AIMP1 can be localized to the ER lumen, because secretory proteins and membrane proteins are transported via ER-Golgi secretory pathway. The present study demonstrates that high proportions of AIMP1 are localized to the ER and lesser extent to Golgi (Figure 2).

It was found during this work that AIMP1 uses different domains for binding gp96 (Figure 1G) and tRNA synthetase.² The gp96-binding region of AIMP1 (amino acids 54 to 192) contains lysine-rich sequences and the C-terminal dimerization domain of gp96 contains glutamic acid-rich sequences. Furthermore, the gp96 E791Δ variant showed less affinity for AIMP1 than WT protein (Supplementary Figure 2 at <http://ajp.amjpathol.org>), suggesting the possibility that the charge-charge interaction is involved in their association. The pH-dependent interaction of AIMP1 and gp96 (Figure 1F) further supports this possibility.

Although it is not known whether the KDEL receptor forms a dimer, KDEL-containing proteins such as Bip, PDI, and gp96 are known to form dimers.^{42,62,63} Furthermore, AIMP1 can form a dimer^{44,45} and promote gp96 dimer formation (Figure 3, A and B) and complex formation between gp96 and KDEL-1 (Figure 3, C and D), suggesting that there is a possibility that AIMP1 dimer promotes the dimerization of gp96 and then assists in the anchoring of gp96 dimer to KDEL-1.

The association between AIMP1 and gp96 showed a striking sensitivity to pH change with maximum affinity at pH 5 (Figure 1F). The binding of KDEL ligand and receptor is also responsive to pH change and requires an

acidic pH.³¹ This suggests that complex formation between AIMP1 and gp96 and KDEL receptor may be controlled by pH difference between the ER and Golgi. As mentioned above, ER has a neutral pH,⁶⁴ and Golgi has been reported to contain a proton pump⁶⁵ and to have a lower pH than the ER. Therefore, there is a possibility that AIMP1-bound gp96 has a higher affinity for KDEL receptor in the Golgi. Thus, the AIMP1/gp96/KDEL receptor complex is likely to be formed in the Golgi and returned to the ER and then dissociate. However, it is not known whether this pH difference affects the dimerization of AIMP1 and gp96.

The deletion of glutamic acid near the C-terminal KDEL sequence of gp96 reduced AIMP1 binding (Supplementary Figure 2 at <http://ajp.amjpathol.org>). This C-terminal glutamic acid-rich region of gp96 was not observed in other KDEL-containing proteins, and the subcellular localization of GRP78/Bip was no difference in AIMP1-deficient cells (data not shown), suggesting that AIMP1 has a specific function for gp96 although the reason why gp96 specifically requires AIMP1 for its retrieval still remains to be determined.

In AIMP1-deficient cells, gp96 localized at the cell surface (Figure 4, C-F), but it has not been determined how the cell surface localization of gp96 is achieved, because gp96 has neither a transmembrane domain nor a glycosylphosphatidylinositol (GPI) anchor site for attachment to the plasma membrane. It is possible that an adaptor molecule is required for the cell surface localization of gp96. In a previous report, KDEL-containing calreticulin at the cell surface was found to use CD59 as an adaptor molecule,⁶⁶ which supports this possibility.

Our mechanistic study demonstrated that AIMP1, by directly forming a complex with gp96, is responsible for preventing its cell surface presentation. Thus, AIMP1^{-/-} mice show increased gp96 cell surface expression, which could result in DC hyperactivation and the development of autoimmune diseases. Several pieces of evidence support this notion. First, the silencing of gp96 by siRNA in AIMP1^{-/-} cells abrogated DC maturation by AIMP1^{-/-} APCs (Figure 6). Second, transgenic mice overexpressing membrane-bound gp96 developed systemic autoimmune diseases.²⁶ Specifically, the autoimmune phenotypes of AIMP1^{-/-} mice included ANA, glomerulonephritis, hypergammaglobulinemia, and immune cell infiltrations (Figure 7), and these are remarkably similar to those of gp96tm-Tg mice. Third, like 96tm-Tg mice, AIMP1^{-/-} mice showed no gross alteration of the hematopoietic system, although they did have more matured DCs in secondary lymphoid organs (Figure 5), suggesting that the autoimmune phenotype in both models is attributable to a breakdown of DC-mediated peripheral tolerance. Fourth, further increases in the expression of cell surface gp96, as in the case of double-mutant 96tm⁺ AIMP1^{-/-} mice (data not shown), resulted in markedly more severe disease, although both 96tm-Tg and AIMP1^{-/-} mice developed autoimmune diseases, they survived for at least 6 months, whereas AIMP1^{-/-} 96tm⁺ mice showed much higher levels of mortality (8 of 44 pups died at age 3 to 4 weeks). Histological analysis of double mutants revealed no significant hepatospleno-

megaly or lymphadenopathy, but they were found to show severe necrotizing enterocolitis, which is consistent with the overwhelming sepsis (data not shown). Combined together, the findings of this study suggest that AIMP1 is a critical regulator of the ER retention of gp96 and that disruption of the interaction between these two molecules might be a key component of pathogenic pathways that lead to the development of systemic autoimmune diseases like lupus.

References

1. Quevillon S, Agou F, Robinson JC, Mirande M: The p43 component of the mammalian multi-synthetase complex is likely to be the precursor of the endothelial monocyte-activating polypeptide II cytokine. *J Biol Chem* 1997, 272:32573–32579
2. Park SG, Jung KH, Lee JS, Jo YJ, Motegi H, Kim S, Shiba K: Precursor of pro-apoptotic cytokine modulates aminoacylation activity of tRNA synthetase. *J Biol Chem* 1999, 274:16673–16676
3. Lee SW, Cho BH, Park SG, Kim S: Aminoacyl-tRNA synthetase complexes: beyond translation. *J Cell Sci* 2004, 117:3725–3734
4. Park SG, Ewalt K, Kim S: Functional expansion of aminoacyl-tRNA synthetases and their interacting factors: new perspectives on housekeepers. *Trends Biochem Sci* 2005, 30:569–574
5. Kim Y, Shin J, Li R, Cheing C, Kim K, Kim S: A novel anti-tumor cytokine contains an RNA binding motif present in aminoacyl-tRNA synthetases. *J Biol Chem* 2000, 275:27062–27068
6. Ko YG, Park H, Kim T, Lee JW, Park SG, Seol W, Kim JE, Lee WH, Kim SH, Park JE, Kim S: A cofactor of tRNA synthetase, p43, is secreted to up-regulate proinflammatory genes. *J Biol Chem* 2001, 276:23028–23033
7. Park H, Park SG, Lee JW, Kim T, Kim G, Ko YG, Kim S: Monocyte cell adhesion induced by a human aminoacyl-tRNA synthetase associated factor, p43: identification of the related adhesion molecules and signal pathways. *J Leukoc Biol* 2002, 71:223–230
8. Park H, Park G, Kim J, Ko YG, Kim S: Signaling pathways for TNF production induced by human aminoacyl-tRNA synthetase-associated factor, p43. *Cytokine* 2002, 20:148–153
9. Park SG, Kang YS, Ahn YH, Lee SH, Kim KR, Kim KW, Koh GY, Ko YG, Kim S: Dose-dependent biphasic activity of tRNA synthetase-associated factor, AIMP1, in angiogenesis. *J Biol Chem* 2002, 277:45243–45248
10. Park SG, Shin HS, Shin YK, Lee Y, Choi EC, Park BJ, Kim S: The novel cytokine p43 stimulates dermal fibroblast proliferation and wound repair. *Am J Pathol* 2005, 166:387–398
11. Park SG, Kang YS, Kim JY, Ko YG, Lee WJ, Lee KU, Kim S: Hormonal activity of AIMP1/p43 for glucose homeostasis. *Proc Natl Acad Sci USA* 2006, 103:14913–14918
12. Wolfe CL, Warrington JA, Davis S, Green S, Norcum MT: Isolation and characterization of human nuclear and cytosolic multisynthetase complexes and the intracellular distribution of p43/EMAPII. *Protein Sci* 2003, 12:2282–2290
13. Li Z, Dai J, Zheng H, Liu B, Caudill M: An integrated view of the roles and mechanisms of heat shock protein gp96-peptide complex in eliciting immune response. *Front Biosci* 2002, 7:d731–d751
14. Koch G, Smith M, Macer D, Webster P, Mortara R: Endoplasmic reticulum contains a common, abundant calcium-binding glycoprotein, endoplasmic reticulum chaperone. *J Cell Sci* 1986, 86:217–232
15. Altmeyer A, Maki RG, Feldweg AM, Heike M, Prottopopov VP, Masur SK, Srivastava PK: Tumor-specific cell surface expression of KDEL-containing, endoplasmic reticular heat shock protein gp96. *Int J Cancer* 1996, 69:340–349
16. Wiest D, Bhandoola A, Punt J, Kreibich G, McKean D, Singer A: Incomplete endoplasmic reticulum (ER) retention in immature thymocytes as revealed by surface expression of "ER-resident" molecular chaperones. *Proc Natl Acad Sci USA* 1997, 94:1884–1889
17. Srivastava PK, Menoret A, Basu S, Binder RJ, McQuade KL: Heat shock proteins come of age: primitive functions acquire new roles in an adaptive world. *Immunity* 1998, 8:657–665
18. Srivastava PK: Roles of heat-shock proteins in innate and adaptive immunity. *Nat Rev Immunol* 2002, 2:185–194
19. Hilf N, Singh-Jasuja H, Schwarzmaier P, Gouttefangeas C, Rammensee HG, Schild H: Human platelets express heat shock protein receptors and regulate dendritic cell maturation. *Blood* 2002, 99:3676–3682
20. Basu S, Binder RJ, Suto R, Anderson KM, Srivastava PK: Necrotic but not apoptotic cell death releases heat shock proteins, which deliver a partial maturation signal to dendritic cells and activate the NF-kappa B pathway. *Int Immunol* 2000, 12:1539–1546
21. Banerjee PP, Vinay DS, Mathew A, Raju M, Parekh V, Prasad DV, Kumar A, Mitra D, Mishra GC: Evidence that glycoprotein 96 (B2), a stress protein, functions as a Th2-specific costimulatory molecule. *J Immunol* 2002, 169:3507–3518
22. Binder RJ, Han DK, Srivastava PK: CD91: a receptor for heat shock protein gp96. *Nat Immunol* 2000, 1:151–155
23. Basu S, Binder RJ, Ramalingam T, Srivastava PK: CD91 is a common receptor for heat shock proteins gp96, hsp90, hsp70, and calreticulin. *Immunity* 2001, 14:303–313
24. Vabulas RM, Braedel S, Hilf N, Singh-Jasuja H, Herter S, Ahmad-Nejad P, Kirschning CJ, Da Costa C, Rammensee HG, Wagner H, Schild H: The endoplasmic reticulum-resident heat shock protein gp96 activates dendritic cells via the Toll-like receptor 2/4 pathway. *J Biol Chem* 2002, 277:20847–20853
25. Singh-Jasuja H, Scherer HU, Hilf N, Arnold-Schild D, Rammensee HG, Toes RE, Schild H: The heat shock protein gp96 induces maturation of dendritic cells and down-regulation of its receptor. *Eur J Immunol* 2000, 30:2211–2215
26. Liu B, Dai J, Zheng H, Stoilova D, Sun S, Li Z: Cell surface expression of an endoplasmic reticulum resident heat shock protein gp96 triggers MyD88-dependent systemic autoimmune diseases. *Proc Natl Acad Sci USA* 2003, 100:15824–15829
27. Lewis MJ, Pelham HR: A human homologue of the yeast HDEL receptor. *Nature* 1990, 348:162–163
28. Semenza JC, Hardwick KG, Dean N, Pelham HR: ERD2, a yeast gene required for the receptor-mediated retrieval of luminal ER proteins from the secretory pathway. *Cell* 1990, 61:1349–1357
29. Griffiths G, Ericsson M, Krijnse-Locker J, Nilsson T, Goud B, Soling HD, Tang BL, Wong SH, Hong W: Localization of the Lys, Asp, Glu, Leu tetrapeptide receptor to the Golgi complex and the intermediate compartment in mammalian cells. *J Cell Biol* 1994, 127:1557–1574
30. Lewis MJ, Pelham HR: Ligand-induced redistribution of a human KDEL receptor from the Golgi complex to the endoplasmic reticulum. *Cell* 1992, 68:353–364
31. Wilson DW, Lewis MJ, Pelham HR: pH-dependent binding of KDEL to its receptor in vitro. *J Biol Chem* 1993, 268:7465–7468
32. Kim Y, Kim JE, Lee SD, Lee TG, Kim JH, Park JB, Han JM, Jang SK, Suh PG, Ryu SH: Phospholipase D1 is located and activated by protein kinase C alpha in the plasma membrane in 3Y1 fibroblast cell. *Biochim Biophys Acta* 1999, 1436:319–330
33. Sampath P, Mazumder B, Seshadri V, Gerber C, Chavatte L, Kinder MT, Dignam JD, Kim S, Driscoll DM, Fox PL: Non-canonical translational silencing activity of glutamyl-prolyl-tRNA synthetase. *Cell* 2004, 119:195–208
34. Ko YG, Kang YS, Kim EK, Park SG, Kim S: Nucleolar localization of human methionyl-tRNA synthetase and its role in ribosomal RNA synthesis. *J Cell Biol* 2000, 149:567–574
35. Ko YG, Kim EK, Kim T, Park H, Park HS, Choi EJ, Kim S: Glutamine-dependent antiapoptotic interaction of human glutaminyl-tRNA synthetase with apoptosis signal-regulating kinase 1. *J Biol Chem* 2001, 276:6030–6036
36. Park SG, Kim HJ, Min YH, Choi EC, Shin YK, Park BJ, Lee SW, Kim S: Human lysyl-tRNA synthetase is secreted to trigger pro-inflammatory response. *Proc Natl Acad Sci USA* 2005, 102:6356–6361
37. Halwani R, Cen S, Javanbakht H, Saadatmand J, Kim S, Shiba K, Kleiman L: Cellular distribution of lysyl-tRNA synthetase and its interaction with gag during human immunodeficiency virus type 1 assembly. *J Virol* 2004, 78:7553–7564
38. Kim MJ, Park BJ, Kang YS, Kim HJ, Park JH, Kang JW, Lee SW, Han JM, Lee HW, Kim S: Downregulation of fuse-binding protein and c-myc by tRNA synthetase cofactor, p38/JTV-1, for lung differentiation. *Nat Genet* 2003, 34:330–336
39. Ko HS, Coelln R, Sriram SR, Kim SW, Chung KKK, Pletnikova O, Troncoso J, Johnson B, Saffary R, Goh EL, Song H, Park BJ, Kim MJ,

- Kim S, Dawson VL, Dawson TM: Accumulation of the authentic Parkin substrate aminoacyl-tRNA synthetase cofactor, p38/JTV-1, leads to catecholaminergic cell death. *J Neurosci* 2005, 25:7968–7978
40. Park BJ, Kang JW, Lee SW, Choi SJ, Shin YK, Ahn YH, Choi YH, Choi D, Lee KS, Kim S: The haploinsufficient tumor suppressor p18 up-regulates p53 via interactions with ATM/ATR. *Cell* 2005, 120:209–221
41. Han JM, Park SG, Lee Y, Kim S: Structural separation of different extracellular activities in aminoacyl-tRNA synthetase-interacting multi-functional protein, p43/AIMP1. *Biochem Biophys Res Commun* 2006, 342:113–118
42. Wearsch PA, Nicchitta CV: Purification and partial molecular characterization of GRP94, an ER resident chaperone. *Protein Expr Purif* 1996, 7:114–121
43. Minami Y, Kawasaki H, Miyata Y, Suzuki K, Yahara I: Analysis of native forms and their isoform compositions of the mouse 90-kDa heat-shock protein, HSP90. *J Biol Chem* 1991, 266:10099–10103
44. Quevillon S, Robinson JC, Berthonneau E, Siatecka M, Mirande M: Macromolecular assemblage of aminoacyl-tRNA synthetases: identification of protein-protein interactions and characterization of a core protein. *J Mol Biol* 1999, 285:183–195
45. Wolfe CL, Warrington JA, Treadwell L, Norcum MT: A three-dimensional working model of the multienzyme complex of aminoacyl-tRNA synthetases based on electron microscopic placements of tRNA and proteins. *J Biol Chem* 2005, 280:38870–38878
46. Aoe T, Lee AJ, van Donselaar E, Peters PJ, Hsu VW: Modulation of intracellular transport by transported proteins: insight from regulation of COPI-mediated transport. *Proc Natl Acad Sci USA* 1998, 95:1624–1629
47. Baker-LePain JC, Sarzotti M, Fields TA, Li CY, Nicchitta CV: GRP94 (gp96) and GRP94 N-terminal geldanamycin binding domain elicit tissue nonrestricted tumor suppression. *J Exp Med* 2002, 196:1447–1459
48. Yamazaki K, Nguyen T, Podack ER: Cutting edge: tumor secreted heat shock-fusion protein elicits CD8 cells for rejection. *J Immunol* 1999, 163:5178–5182
49. de Crom R, van Haperen R, Janssens R, Visser P, Willemsen R, Grosveld F, van der Kamp A: Gp96/GRP94 is a putative high density lipoprotein-binding protein in liver. *Biochim Biophys Acta* 1999, 1437:378–392
50. Morales H, Muharemagic A, Gantress J, Cohen N, Robert J: Bacterial stimulation upregulates the surface expression of the stress protein gp96 on B cells in vivo: distinct function, phenotype, and localization of dendritic cell subsets in FLT3 ligand-treated mice. *J Immunol* 1997, 159:2222–2231
51. Pulendran B, Lingappa J, Kennedy MK, Smith J, Teepe M, Rudensky A, Maliszewski CR, Maraskovsky E: Developmental pathways of dendritic cells in vivo: distinct function, phenotype, and localization of dendritic cell subsets in FLT3 ligand-treated mice. *J Immunol* 1997, 159:2222–2231
52. Hanada T, Tanaka K, Matsumura Y, Yamauchi M, Nishinakamura H, Aburatani H, Mashima R, Kubo M, Kobayashi T, Yoshimura A: Induction of hyper Th1 cell-type immune responses by dendritic cells lacking the suppressor of cytokine signaling-1 gene. *J Immunol* 2005, 174:4325–4332
53. Randow F, Seed B: Endoplasmic reticulum chaperone gp96 is required for innate immunity but not cell viability. *Nat Cell Biol* 2001, 3:891–896
54. Steinman RM, Nussenzweig MC: Avoiding horror autotoxicus: the importance of dendritic cells in peripheral T cell tolerance. *Proc Natl Acad Sci USA* 2002, 99:351–358
55. Liu K, Iyoda T, Saternus M, Kimura Y, Inaba K, Steinman RM: Immune tolerance after delivery of dying cells to dendritic cells in situ. *J Exp Med* 2002, 196:1091–1097
56. Belz GT, Behrens GM, Smith CM, Miller JF, Jones C, Lejon K, Fathman CG, Mueller SN, Shortman K, Carbone FR, Heath WR: The CD8alpha(+) dendritic cell is responsible for inducing peripheral self-tolerance to tissue-associated antigens. *J Exp Med* 2002, 196:1099–1104
57. Hawiger D, Inaba K, Dorsett Y, Guo M, Mahnke K, Rivera M, Ravetch JV, Steinman RM, Nussenzweig MC: Dendritic cells induce peripheral T cell unresponsiveness under steady state conditions in vivo. *J Exp Med* 2001, 194:769–779
58. Turley SJ: Dendritic cells: inciting and inhibiting autoimmunity. *Curr Opin Immunol* 2002, 14:765–770
59. Green EA, Eynon EE, Flavell RA: Local expression of TNF-alpha in neonatal NOD mice promotes diabetes by enhancing presentation of islet antigens. *Immunity* 1998, 9:733–743
60. Hori S, Nomura T, Sakaguchi S: Control of regulatory T cell development by the transcription factor Foxp3. *Science* 2003, 299:1057–1061
61. Zheng H, Dai J, Stoilova D, Li Z: Cell surface targeting of heat shock protein gp96 induces dendritic cell maturation and antitumor immunity. *J Immunol* 2001, 167:6731–6735
62. Carlino A, Toledo H, Skaleris D, DeLisio R, Weissbach H, Brot N: Interactions of liver Grp78 and Escherichia coli recombinant Grp78 with ATP: multiple species and disaggregation. *Proc Natl Acad Sci USA* 1992, 89:2081–2085
63. Quéméneur E, Guthapfel R, Gueguen P: A major phosphoprotein of the endoplasmic reticulum is protein disulfide isomerase. *J Biol Chem* 1994, 269:5485–5488
64. Mellman I, Fuchs R, Helenius A: Acidification of the endocytic and exocytic pathways. *Annu Rev Biochem* 1986, 55:663–700
65. Glickman J, Croen K, Kelly S, Al-Awqati Q: Golgi membranes contain an electrogenic H⁺ pump in parallel to a chloride conductance. *J Cell Biol* 1983, 97:1303–1308
66. Ghiran I, Klickstein LB, Nicholson-Weller A: Calreticulin is at the surface of circulating neutrophils and uses CD59 as an adaptor molecule. *J Biol Chem* 2003, 278:21024–21031